# Characterization of thiol-based redox modifications of *Brassica napus* SNF1-related protein kinase 2.6-2C

Tianyi Ma[1,2,3], Mi-Jeong Yoo[2], Tong Zhang[2], Lihong Liu[2], Jin Koh[4], Wen-Yuan Song[5,6], Alice C. Harmon[2,6], Wei Sha[1,3] and Sixue Chen[2,4,6]

1 College of Life Sciences, Northeast Forestry University, Harbin, China
2 Department of Biology, Genetics Institute, University of Florida, Gainesville, FL, USA
3 College of Life Sciences, Agriculture and Forestry, Qiqihar University, Heilongjiang, China
4 Proteomics and Mass Spectrometry, Interdisciplinary Center for Biotechnology Research, University of Florida, Gainesville, FL, USA
5 Department of Plant Pathology, University of Florida, Gainesville, FL, USA
6 Plant Molecular and Cellular Biology, University of Florida, Gainesville, FL, USA

Sucrose nonfermenting 1-related protein kinase 2.6 (SnRK2.6), also known as Open Stomata 1 (OST1) in *Arabidopsis thaliana*, plays a pivotal role in abscisic acid (ABA)-mediated stomatal closure. Four *SnRK2.6* paralogs were identified in the *Brassica napus* genome in our previous work. Here we studied one of the paralogs, *BnSnRK2.6-2C*, which was transcriptionally induced by ABA in guard cells. Recombinant BnSnRK2.6-2C exhibited autophosphorylation activity and its phosphorylation sites were mapped. The autophosphorylation activity was inhibited by S-nitrosoglutathione (GSNO) and by oxidized glutathione (GSSG), and the inhibition was reversed by reductants. Using monobromobimane (mBBr) labeling, we demonstrated a dose-dependent modification of BnSnRK2.6-2C by GSNO. Furthermore, mass spectrometry analysis revealed previously uncharacterized thiol-based modifications including glutathionylation and sulfonic acid formation. Of the six cysteine residues in BnSnRK2.6-2C, C159 was found to have different types of thiol modifications, suggesting its high redox sensitivity and versatility. In addition, mBBr labeling on tyrosine residues was identified. Collectively, these data provide detailed biochemical characterization of redox-induced modifications and changes of the BnSnRK2.6-2C activity.

Crop yield depends largely on $CO_2$ assimilation during photosynthesis, which is accompanied by water loss via transpiration. Both $CO_2$ uptake and water loss occur mainly through stomata, the microscopic pores formed by pairs of guard cells in the leaf epidermis [1–3]. Stomatal opening and closing are responsive to many environmental factors and play a critical role in response to abiotic (e.g., drought) and biotic (e.g., pathogen invasion) stresses [2]. In addition, modulation of stomatal aperture by phytohormones like

**Abbreviations**

$[Ca^{2+}]_{cyt}$, cytosolic $Ca^{2+}$ concentration; ABA, abscisic acid; CBB, Coomassie Brilliant Blue R-250; CDS, coding DNA sequences; cysTMT, cysteine reactive tandem mass tagging; GCP, guard cell protoplasts; Grx, glutaredoxin; GSH, reduced glutathione; GSNO, S-nitrosoglutathione; GSSG, oxidized glutathione; IAM, iodoacetamide; ICAT, isotope-coded affinity tagging; iodoTMT, iodoacetyl tandem mass tagging; IPTG, isopropyl-beta-D-thiogalactopyranoside; mBBr, monobromobimane; MeJA, methyl jasmonate; OST1, open stomata 1; PP2C, phosphatase 2C; PSM, peptide spectrum match; PTM, post-translational modification; RCAR/PYR1/PYL, regulatory component of ABA receptor/pyrabactin resistance 1/pyr1-like; ROS, reactive oxygen species; $RSO_2H$, sulfinic acids; $RSO_3H$, sulfonic acids; RSOH, sulfenic acids; SLAC1, slow anion channel associated 1; SnRK, sucrose nonfermenting 1-related protein kinase.

abscisic acid (ABA) and methyl jasmonate (MeJA) has been well studied [3–9]. For example, both ABA and MeJA activate $Ca^{2+}$ channels and S-type anion channels, leading to an elevated cytosolic $Ca^{2+}$ concentration ($[Ca^{2+}]_{cyt}$) and an increase in the cytosolic pH, which in turn trigger stomatal closure [8,9]. Importantly, both nitric oxide (NO) and reactive oxygen species (ROS) function as second messengers in the ABA- and MeJA-regulated stomatal movement. Similar to ROS, NO regulates $Ca^{2+}$ channels to control cytosolic $Ca^{2+}$ concentration in guard cells [9–12]. The functions of NO, ROS, and other weak oxidants in guard cells have been attributed to their abilities to induce oxidative modifications including S-nitrosylation and S-glutathionylation of key proteins [13–15]. In particular, cysteine residues are prone to such modifications due to their highly active nucleophilic sulfhydryl groups [16], making redox-induced thiol modifications an essential process in cellular signaling [17,18]. Recently, ABA-induced stomatal closure was found to be inhibited by S-nitrosylation of Cys 137 in OPEN STOMATA 1 (OST1, SnRK2.6) in *Arabidopsis thaliana*, a key protein in the guard cell ABA signaling pathway [14,19]. In addition to the Arabidopsis OST1, major changes in S-nitrosylation and S-glutathionylation of a plethora of other proteins have been found to result from abiotic stress-induced ROS production and/or direct oxidant treatment [20,21]. For example, a SnRK2.4 in *Brassica napus* guard cells is redox-modified upon ABA treatment. Additionally, its activity is inhibited by $H_2O_2$, S-nitrosoglutathione (GSNO), and oxidized glutathione (GSSG), and recovered by treatment with dithiothreitol (DTT), implying that ABA may induce reversible redox modification of SnRK2s in guard cells [22].

Models of ABA signaling with many molecular components have been proposed [6,9,23,24], including the OST1 [25–28]. OST1 belongs to a plant-specific kinase group, sucrose nonfermenting 1-related kinase 2 (SnRK2). Other members of the SnRK2 family such as SnRK2.2 and SnRK2.3 can also be activated by ABA, mostly in seed development and dormancy [29–31]. In the absence of ABA, these SnRK2s are bound to clade A PHOSPHATASE 2Cs (PP2Cs) and thus are inhibited. In the presence of ABA, PP2Cs are bound by ABA receptors, RCAR/PYR1/PYL (REGULATORY COMPONENT OF ABA RECEPTOR/PYRABACTIN RESISTANCE 1/PYR1-LIKE), releasing the inhibition of the SnRK2.6 [29,32,33]. Active SnRK2.6 phosphorylates an array of substrates such as bZIP transcription factors [34,35], SLOW ANION CHANNEL ASSOCIATED 1 (SLAC1), and $H^+$-ATPases to induce stomatal

closure [26,36–41]. Similar functions of OST1 were found in maize (*Zea mays*) [42], tomato (*Solanum lycopersicum*) [43], black cottonwood (*Populus trichocarpa*) [44], and cabbage (*Brassica oleracea*) [45]. Interestingly, OST1 was also required in regulating stomatal movement triggered by factors other than ABA, such as red light, yeast elicitor, and $CO_2$ [46,47], making this kinase a convergence point for various stimuli. Furthermore, OST1 also functions in plant drought response [45,48], low temperature response [49–51], seed development and dormancy [52], and fruit ripening[53], suggesting the versatility of the kinase and multiple regulatory mechanisms involved in the different processes.

While the physiological functions of OST1 have been extensively studied, interest in elucidation of the relationship between the kinase and ROS has emerged. It has been demonstrated that OST1 can act either upstream or downstream of ROS in the ABA signaling pathway [54–57]. For example, OST1 can phosphorylate AtRBOH F NADPH oxidase to boost ROS production [58]; oxidant treatment of OST1 can trigger the alteration of its phosphorylation activity *in vitro* [14], indicating that the activity of OST1 could be redox-regulated. However, the molecular mechanism underlying the redox regulation of OST1 is not fully understood. For example, it is not known whether the Cys 137 nitrosylation in Arabidopsis [14] also occurs in other OST homologs, and whether other types of redox modification play a role in the kinase regulation.

We have previously shown that transcripts of two *SnRK2.6* genes, *BnSnRK2.6-2A* (BnaAnng41460D) and *BnSnRK2.6-2C* (BnaC07g00000D), which are highly expressed in *B. napus* guard cells, are induced by ABA and drought [48]. The two SnRK2.6 genes encode the same protein sequence, namely BnSnRK2.6-2C. Although the effect of NO on SnRK2.6 activity has been reported in Arabidopsis [14], a comprehensive investigation of redox regulation of SnRK2.6 from any species has not been conducted. In this study, we focused on the redox regulation of the SnRK2.6-2C from *B. napus*, an important oilseed crop. The activity of recombinant BnSnRK2.6-2C was inhibited by GSSG and GSNO treatments, and the inhibition was reversed by reductant treatment. Different thiol modifications of BnSnRK2.6-2C were identified including sulfonic acids and S-glutathionylation. Interestingly, C159 was identified in all the samples and subjected to various thiol post-translational modifications (PTMs). As C159 is the only cysteine residue in the "activation loop" of the kinase, the biological significance of the PTMs is of interest. The results

reported here form the foundation for further studies of redox regulation of BnSnRK2.6-2C and its C159 in the physiological context of stomatal functions.

## Results

### Structural analysis of BnSnRK2.6-2C, a member of the Group III of SnRK2 family

The coding DNA sequences (CDSs) of *BnSnRK2.6-2C* and *BnSnRK2.6-2A* were cloned from *B. napus* GCPs and sequenced in our previous work, and both genes were highly expressed in GCPs and induced by ABA and drought treatments [48]. CDSs of the two paralogs are identical in length to their *A. thaliana* ortholog *AtOST1* (At4 g33950) (Fig. S1A). In addition, the three coding sequences show 99.2% similarity (Fig. S1A). The deduced amino acid sequences encoded by the *BnSnRK2.6-2C* and *BnSnRK2.6-2A* are identical, and the encoded protein was named as BnSnRK2.6-2C because *BnSnRK2.6-2C* showed higher expression in control and ABA-treated *B. napus* GCPs [48]. As shown in Fig. 1A, BnSnRK2.6-2C belongs to group III of the SnRK2 kinase family with a serine/threonine protein kinase domain containing the activation loop, a SnRK2-specific domain (Domain I) for osmotic stress response, and a group III SnRK2-specific domain (Domain II) for ABA response [59].

Comparison of BnSnRK2.6-2C with AtOST1 shows that the identity of the overall protein sequences and that of the conserved serine/threonine protein kinase domain were 95.6% and 99.3%, respectively, suggesting similar functions of BnSnRK2.6-2C and AtOST1. In addition, six cysteine residues are present in both kinases, and all are located at the same positions within the serine/threonine protein kinase domain (Fig. 1B). Moreover, the location of the six cysteine residues in OST1s is highly conserved from different plant species (Fig. S1B) [42–45,53]. The three-dimensional structure of BnSnRK2.6-2C was predicted using the RaptorX server (http://raptorx.uchicago.edu/) with the X-ray crystal structure of AtOST1 [60] as a reference. As shown in Fig. 1C-i, two α-helices were found in Domain I, and no secondary structure was predicted for Domain II (Note that the structure of domain II was disordered in 3UC4 and not modeled). Four cysteine residues (C107, C131, C203, and C250) are located in α-helices in the large lobe (Fig. 1C-ii, iii, v, vi) with C131, C203, and C250 being buried in the structure (Fig. 1C-iii, v, vi) and C107 on the surface (Fig. 1C-ii.). C137 and C159 are located in loops (Fig. 1C-iii, iv). C137 is on the

surface, while C159 is located in the catalytic cleft. The thiol groups of C107, C137, and C159 are predicted to face the outside of the protein (Fig. 1C-ii, iii, iv), whereas those of C131, C203, and C250 face toward the core (Fig. 1C-iii, v, vi). No disulfide bonds were found between the six cysteines in either the reference or the predicted structures (Fig. 1C). In the structure of the complex between OST1 with the type C protein phosphatase HAB1 (Protein Data Bank ID: 3UJG [61]), the conformation appears to be different and C131 and C159 are very close together, but no disulfide bond between them is noted. C137 is nearby, but its S atom is pointed away from C131 and C159.
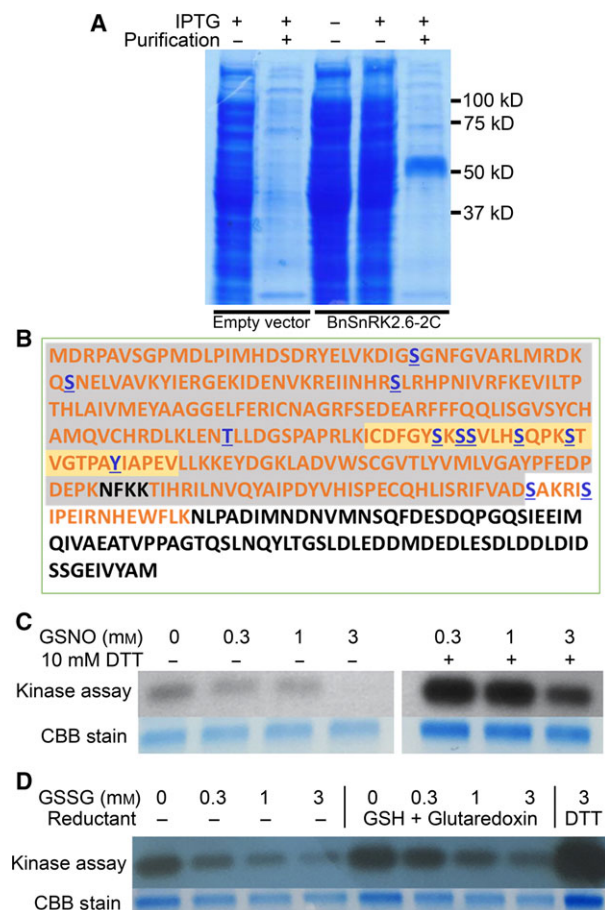
### Redox-regulated autophosphorylation activity of recombinant BnSnRK2.6-2C

Recombinant BnSnRK2.6C was purified, and a dominant band with the predicted size (~ 51 kDa) was observed on SDS/PAGE (Fig. 2A). To validate the identity of the expressed protein and to map its *in vitro* phosphorylation sites, the BnSnRK2.6C protein was subjected to an autophosphorylation reaction followed by digestion with trypsin (EC 3.4.21.4), and the resulting peptides were used for protein identification and phosphorylation site mapping by LC-MS/MS. The identified peptides covered more than 70% of the protein sequence, with 12 phosphorylation sites identified (Fig. 2B, Fig. S2).

To investigate potential redox effects on BnSnRK2.6-2C activity with the consideration of GSH being a main regulator of cellular redox status, two oxidized forms of glutathione, GSSG and GSNO, were used for treatment before performing kinase activity assays. As shown in Fig. 2C,D, the autophosphorylation activity of BnSnRK2.6-2C was suppressed by GSNO and GSSG in a dose-dependent manner. To test whether the oxidant-induced inhibition of kinase activity is reversible, the pre-oxidized samples were further treated either with DTT as a general reductant or with reduced glutathione (GSH) and glutaredoxin (Grx, EC 1.20.4.1) as specific reductants for S-glutathionylation. The results showed that the kinase activity of GNSO- and GSSG-oxidized BnSnRK2.6-2C can be recovered to different extents by the reductants. Compared to the combination of GSH and Grx, DTT showed a stronger effect in enhancing the kinase activity. It was also noteworthy that BnSnRK2.6-2C without oxidant treatment showed an increase in activity by reductant, indicating that a more reducing environment favors the active form of the kinase.
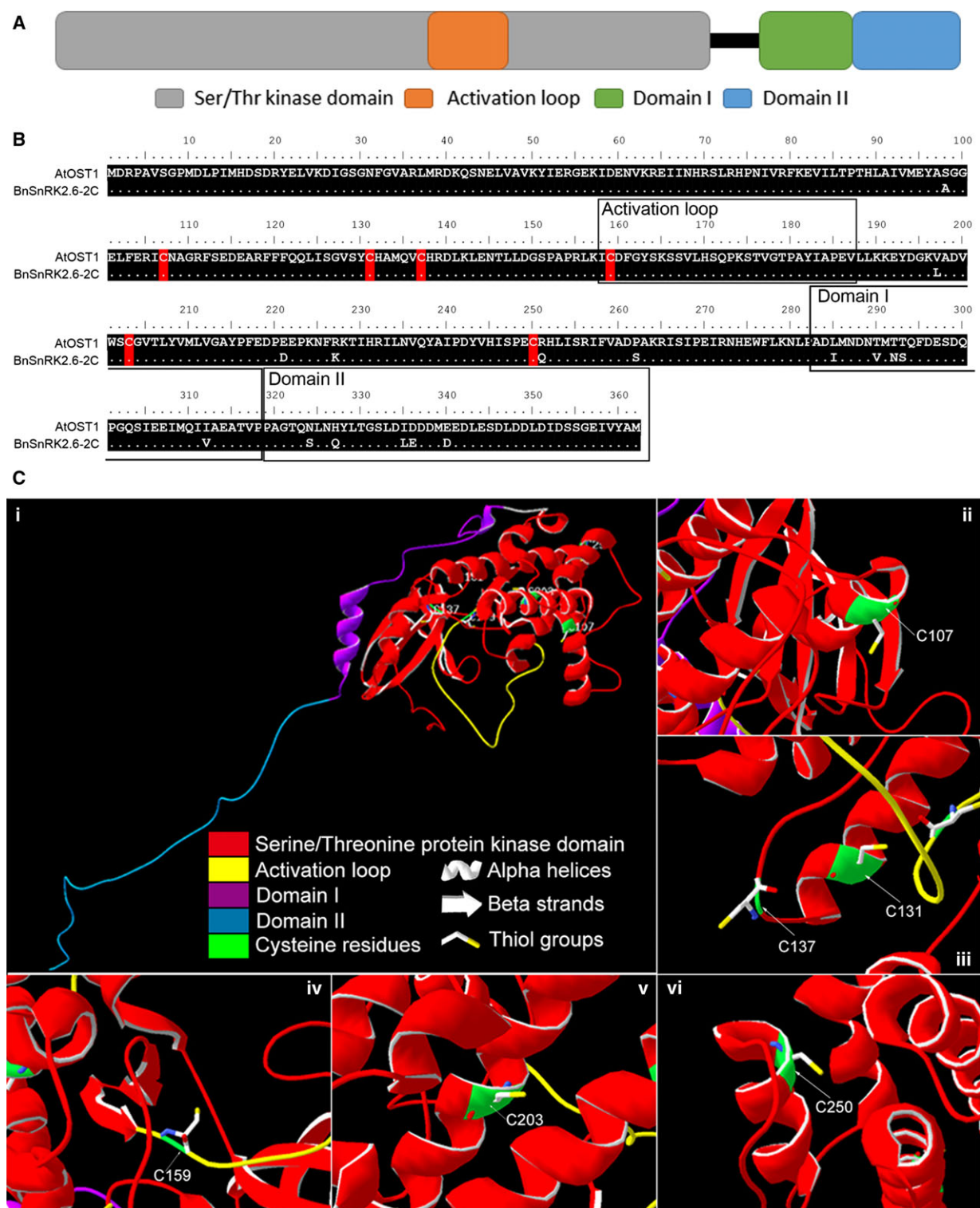
**Fig. 1.** Structural analysis of BnSnRK2.6-2C. (A) Conserved domains of BnSnRK2.6-2C. A serine/threonine protein kinase domain with activation loop, a SnRK2-specific domain (Domain I) and a SnRK2, group III-specific domain (Domain II) were predicted. (B) Comparison of amino acids sequences of BnSnRK2.6-2C and AtOST1 (At4g33950). Sequences of conserved domains are shown in boxes, and locations of cysteine residues are labeled in red. (C) Prediction of the tertiary structure of BnSnRK2.6-2C. Different secondary structures are shown in cartoon, and domains are shown in different colors (i); cysteine residues and thiol groups are labeled in (ii) to (vi).

**Fig. 2.** Autophosphorylation and redox regulation of recombinant BnSnRK2.6-2C. (A) Expression and purification of recombinant BnSnRK2.6-2C. Empty pET28a vector was used as control. (B) Peptides and phosphorylation sites of BnSnRK2.6-2C identified by LC-MS/MS. Sequences of peptides identified are shown in orange, and phosphorylation sites identified are shown in blue with underlines. The serine/threonine protein kinase domain is shaded in gray with the activation loop shaded in yellow. (C) Autophosphorylation activity of BnSnRK2.6-2C treated with GSNO and/or DTT. Upper panel: autoradiograph of BnSnRK2.6-2C. Lower panel: Coomassie Blue staining as loading control. (D) Autophosphorylation activity of BnSnRK2.6-2C treated with GSSG and/or GSH with glutaredoxin or DTT. Upper panel: autoradiograph of BnSnRK2.6-2C. Lower panel: Coomassie Blue staining as loading control.

## Detection of cysteine modifications in BnSnRK2.6-2C by mBBr fluorescence

To further confirm that GSSG- and GSNO-induced modifications on cysteine residues, mBBr labeling was used to study the redox status of the thiol groups of BnSnRK2.6-2C. A forward labeling strategy, in which free thiols available after oxidant and/or reductant treatments were labeled with mBBr directly, was

followed to determine incorporation of mBBr and thus the state of free thiols (Fig. 3A). In this strategy, the intensity of the mBBr fluorescence signal under UV is inversely proportional to the number of cysteines modified by the oxidants. As inferred from the kinase activity data, application of GSNO led to a significant drop in the free thiol content of BnSnRK2.6-2C, which was restored to the original level by DTT (Fig. 3B,D). These data suggest that GSNO causes reversible cysteine modifications. In contrast, no significant changes in mBBr labeling patterns were observed in the GSSG-treated samples compared to untreated control (Fig. 3C,E). Initially, it was thought that the GSSG concentration used in the assays might not be high enough to reveal the differences. However, even a treatment with 24 mM GSSG did not lead to significant changes in the fluorescence signal (data not shown). Clearly, GSSG treatment caused cysteine PTMs based on the mass spectrometry results (Table 1). This result may indicate the limitation of the mBBr method used here.

## Multiple cysteine modifications of BnSnRK2.6-2C identified by LC-MS/MS

To map the oxidant-induced modifications of BnSnRK2.6-2C, LC-MS/MS was used to determine cysteine modifications. Because cysteine modifications including S-nitrosylation and S-glutathionylation may be unstable in the MS assay, a reverse labeling method was used to determine which cysteine residues were reversibly oxidized (Materials and methods, Fig. S3). In this case, the detection of mBBr labeling indicates that the cysteine-containing peptides undergo reversible modifications caused by the oxidants. To ensure the efficiency of mBBr labeling and iodoacetamide (IAM) alkylation, a positive control with neither oxidant treatment nor IAM alkylation before mBBr labeling, and a negative control with DTT treatment before alkylation were added (Table 1, Fig. S3).

Table 1 summarizes the identified modifications, which were labeling by IAM or mBBr; glutathionylation; and oxidation of cysteine residues to sulfinic (–SO₂H) or sulfonic (–SO₃H) acids. Overall, each of the five peptides (including all six cysteine residues of BnSnRK2.6-2C) was identified at least once, revealing several previously unknown modifications of BnSnRK2.6-2C. First, not all the cysteine residues were labeled with mBBr in the positive control. This was expected, given that some cysteine residues may have been inaccessible or oxidized before the assay (Table 1), as indicated by the enhanced kinase activity following DTT treatment (Fig. 2D). In contrast, all
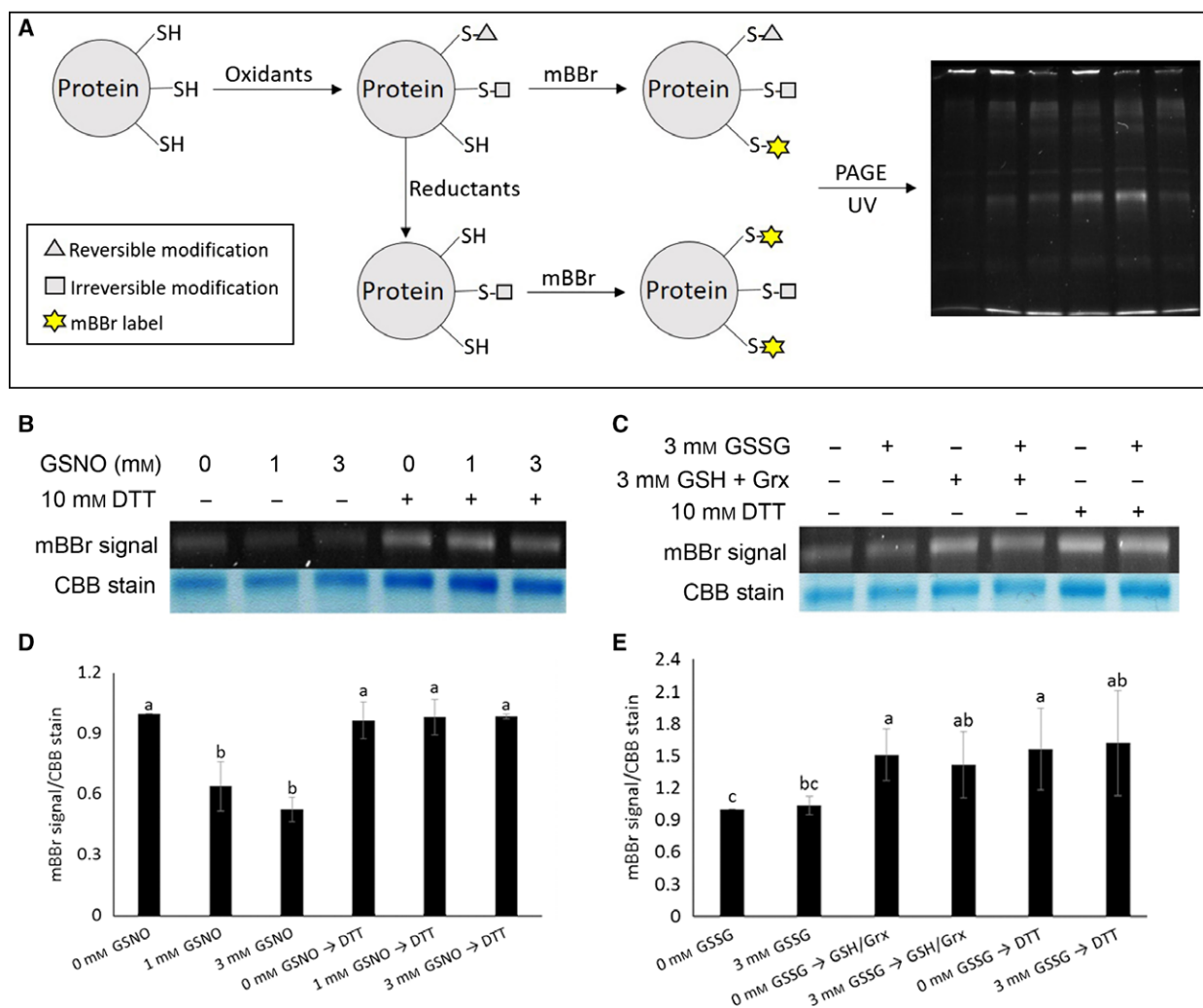
**Fig. 3.** Reversible cysteine thiol oxidation occurred in BnSnRK2.6-2C treated with GSNO or GSSG. (A) Forward mBBr labeling strategy workflow for detecting reversible cysteine thiol oxidation. Treatment of proteins with oxidants resulted in oxidation of some sulfhydryl groups (triangles or squares). Following removal of the oxidant, mBBr was used to label the free thiols (SH). Alternatively, the protein was treated with reductant, and some oxidized sulfhydryls (triangles) were returned to the reduced state (SH), while others remained blocked (squares). Subsequent treatment of protein with mBBr resulted in the modification of sulfhydryls by the reagent, and proteins with mBBr modifications appeared as fluorescent bands on UV-illuminated gels. Reversible cysteine thiol oxidation occurred in BnSnRK2.6-2C treated with GSNO (B) or GSSG (C). Upper panel: UV fluorescence of mBBr-labeled BnSnRK2.6-2C. Lower panel: Coomassie Blue staining as loading control. Relative quantification of mBBr fluorescence of BnSnRK2.6-2C treated with GSNO (D) or GSSG (E). Fluorescence was determined by fluorescence intensity divided by the intensity of Coomassie Blue stain calculated by ImageJ software; values of 0 mM GSNO and 0 mM GSSG treatments were normalized as 1, respectively. Three replicates were used for statistical analysis, Duncan method was used in one-way ANOVA analysis, $P < 0.05$, and standard errors were indicated.

the cysteine residues were found to be alkylated in the negative control (with the absence of unmodified cysteine residues), demonstrating that robust reduction and alkylation occurred. The reliability of mBBr labeling and IAM alkylation was validated by manually inspecting the MS2 spectra with representative spectra shown in Fig. 4A,B, and Fig. S4. Furthermore, cysteine modifications that were previously ignored or

regarded as unstable for MS analysis were successfully identified in this study. For example, oxidation of cysteine residues to sulfonic acid, an irreversible modification rarely taken into consideration, was found in all samples (Fig. 4C, Table 1, Fig. S4). Interestingly, peptides with cysteine S-glutathionylation were directly detected by MS/MS (Fig. 4D, Fig. S4). S-glutathionylation was previously detected in indirect labeling

**Table 1.** Overview of peptides with cysteine thiol modifications in different redox treatments. The percentage in parenthesis represents the fraction of peptide spectral matches (PSMs) of the peptides containing modified cysteine residues relative to the total PSMs of BnSnRK2.6-2C. Positive control: The protein was reduced with DTT, labeled with mBBr directly, and then treated with IAM. Negative control: DTT-reduced free thiols were blocked with IAM before the mBBr labeling. DTT control: The protein was blocked with IAM, then reduced with DTT and labeled with mBBr. GSH control: The protein was blocked with IAM and then reduced with GSH and Grx, followed by mBBr labeling. GSNO, GSSG, and GSSG + GSH treatments (reverse labeling): After the treatment, IAM was used to block the remaining free thiol groups. Reversibly oxidized cysteine residues were then reduced with DTT or GSH and Grx, followed by mBBr labeling.

| | Positive control | Negative control | DTT control | GSH control | GSNO treatment | GSSG treatment | GSSG + GSH treatment |
|---|---|---|---|---|---|---|---|
| IAM | C159 (0.21%)[a] | C107 (0.57%) C131 (0.13%) C137 (0.13%) C159 (9.19%) C203 (0.26%) C250 (0.77%) | C107 (0.25%) C159 (8.72%) | C107 (0.07%) C159 (6.88%) | C107 (0.18%) C159 (4.21%) | C159 (5.32%) C203 (0.12%) | C159 (5.75%) C250 (0.64%) |
| mBBr | C107 (0.53%) C159 (7.22%) | | C159 (0.20%) | C159 (0.60%) | C159 (0.57%) | C131 (0.11%)[b] C137 (0.11%)[b] C159 (0.84%) | C131 (0.20%)[b] C137 (0.20)[b] C159 (0.51%) |
| Glutathionylation | | | | C159 (0.27%) | C107 (0.30%) C159 (0.79%) | C159 (1.27%) | C159 (0.63%) C250 (0.12%)[b] |
| Sulfinic/sulfonic acid | C159 (0.07%) | C159 (0.13%) | C159 (0.50%) | C159 (0.39%) | C159 (0.38%) | C159 (0.42%) | C159 (0.17%) |

[a] Numbers in brackets are percentages of the PSMs of peptides containing modified cysteine residues over the total PSMs of the recombinant BnSnRK2.6-2C in different treatments.
[b] Indicates cysteine-containing peptides detected by LC-MS/MS but the quality of MS2 spectra was of relatively low confidence. All the data represent average of four replicates.

methods or at least after enrichment of glutathiony-lated peptides [62]. However, nitrosylation was not found in our samples on any of the cysteine residues, a result that is in contrast to the report of this modification in AtOST1 [14]. Another interesting observation was that GSNO-treated BnSnRK2.6-2C showed S-glutathionylation modifications on C159 and C107, which were absent in the DTT control. GSNO is known to cause protein nitrosylation, glutathionylation, or both *in vivo* [63]. The reaction may depend on as-yet undetermined features of the microenvironment surrounding the cysteine residues of BnSnRK2.6-2C. S-glutathionylation was also observed in the GSH control and the two GSSG-treated samples, in which the proteins were reduced with either DTT or GSH (Table 1). Thus, these results indicate GSH can lead to cysteine S-glutathionylation, which may not be fully reversed under certain conditions.

We also investigated the possible contribution of the location of cysteine residues to their sensitivity of modifications. Among the six cysteine residues in the protein kinase domain of BnSnRK2.6-2C, C159 was found to be most easily modified (Table 1, Fig. 4). Strikingly, different types of modifications listed in Table 1 can be found in C159-containing peptides. One possible explanation was that C159 was in the flexible activation loop and that the thiol group was

facing outward (Fig. 1C-vi). It was also the only cysteine residue in the activation loop and located in the catalytic cleft (Fig. 1B,C). However, C107, which resides at the surface of the protein (Fig. 1C), showed modifications under the GSNO treatment condition, but not under GSSG treatment (Table 1). The low pKa of cysteine residues is largely determined by the local electrostatic environment; for example, the presence of proximal charged residues such as lysine and arginine residues decreases the pKa [64]. In spite of the scarce distribution of lysine and arginine residues surrounding the other four cysteines, each was identified in at least one sample. Among them, C131, C137, and C250 appeared to be affected by redox, while no modification was detected for C203 located close to the protein core (Fig. S4, Table 1).

## mBBr-labeled tyrosine residues of BnSnRK2.6-2C

Although GSSG treatment clearly led to cysteine modifications (Table 1) and inhibited the BnSnRK2.6-2C activity (Fig. 2D), it did not lead to significant changes in the mBBr fluorescence signal on the gel (Fig. 3E). To further understand the unchanged mBBr fluorescence, the specificity of mBBr labeling was explored. Because tyrosine residues were shown to be labeled by mBBr [65], this modification was considered in the
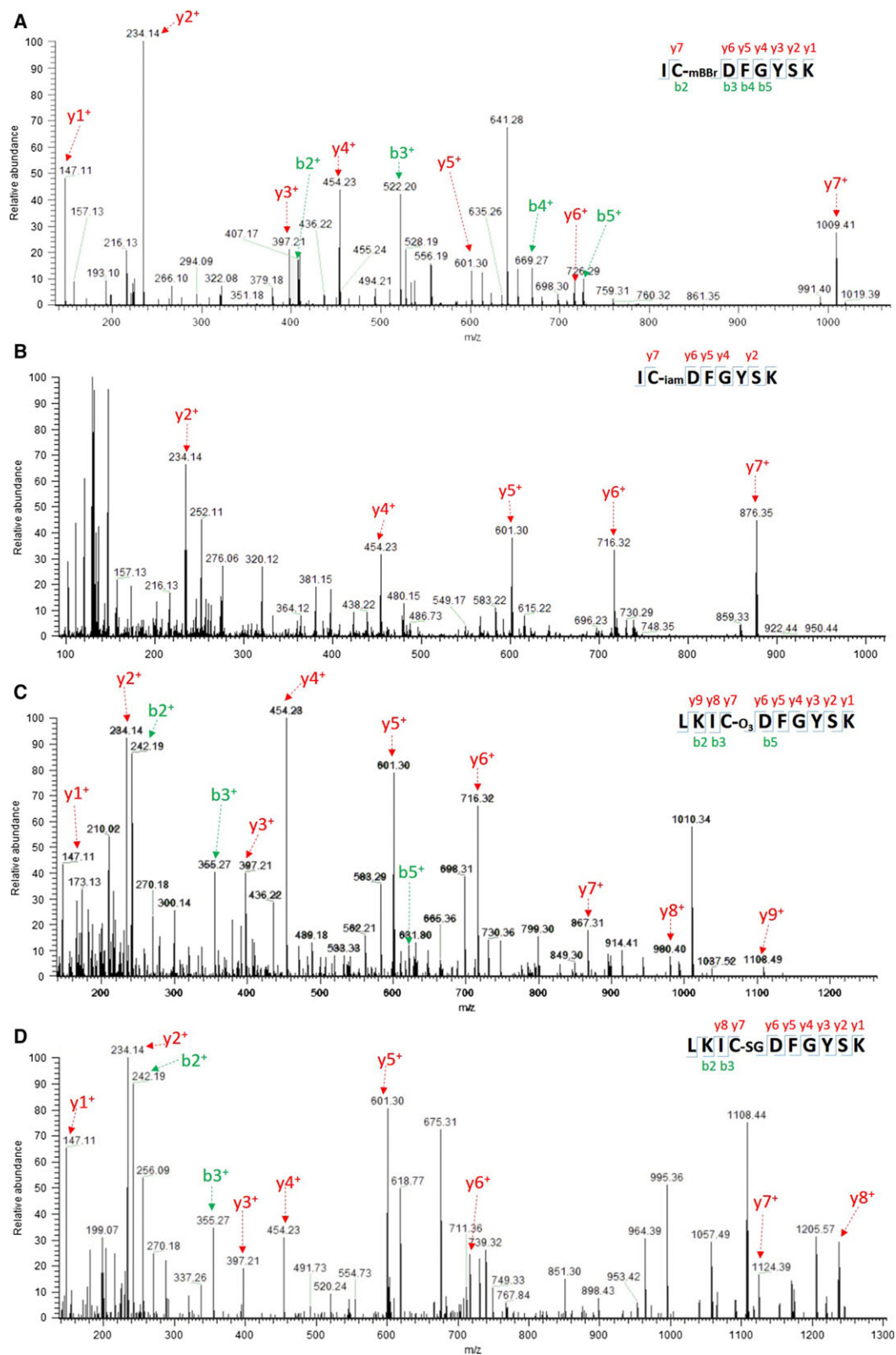
**Fig. 4.** Multiple cysteine thiol modifications detected on C159 of BnSnRK2.6-2C by LC-MS/MS. MS/MS spectra of peptides containing C159 of BnSnRK2.6-2C with mBBr (A), IAM (B), sulfonic acid (C), or glutathione group (D). MS/MS ions used for peptides identification were labeled.

analysis of the MS/MS data. Peptides containing mBBr-labeled tyrosine residues Y51 or Y182 were identified with high confidence in the BnSnRK2.6-2C (Fig. 5A, Fig. S5). Furthermore, the samples with fewer mBBr-labeled cysteine residues seemed to have more mBBr-labeled tyrosine residues (Fig. 5B). Since BnSnRK2.6-2C has 11 tyrosine residues and six cysteine residues, mBBr-labeled tyrosine could have contributed to the overall fluorescence signal of mBBr labeling. However, mBBr-labeled tyrosine residues were not detected in the GSNO-treated samples (Fig. 5B). Such an enigma deserves further investigation and interpretation of GSSG redox protein/proteomics data based on mBBr labeling requires caution.

## Discussion

### BnSnRK2.6-2C is a redox-regulated kinase

Most of the previously identified plant redox-regulated kinases are mitogen-activated protein kinases (MPKs) [66]. For example, oxidants activate MPK1, MPK2 [67], MPK3, MPK4, MPK6 [68–70], and MPK12 [71] in the reference plant *A. thaliana*. Similarly, activation of MPK1, MPK3, and MPK6 in *Oryza sativa* [72,73], MPK3 and MPK5 in *Zea mays* [74,75], and MPK1 and MPK2 in *Solanum lycopersicon* [76] and aggregation of MPK4 in *B. napus* [77] have also been observed. In contrast, other kinases including some MPKs showed decreased activity after oxidation. Recent studies showed that both SnRK2.2 and SnRK2.6 from *Arabidopsis* [14] and SnRK2.4 from *B. napus* [22] are sensitive to redox regulation, with their activities inhibited by oxidants such as GSNO and enhanced by reductants. In this study, BnSnRK2.6-2C autophosphorylation activity was inhibited by GSNO and GSSG in a dose-dependent manner. In addition, the inhibition could be recovered by using the general reductant DTT or specific reductants (GSH and Grx) (Fig. 2C,D). Given the availability of reactive cysteine residues in BnSnRK2.6-2C, cysteine modifications in general were predicted to affect the kinase activity. However, certain cysteine modifications were found in both the oxidant- and reductant-treated samples, in which clear differences in activity were observed (Fig. 4, Fig. S4, Table 1). Hence, it is likely that such modifications may not play a major role in inhibiting the kinase activity. For example, S-glutathionylation on cysteine residues of BnSnRK2.6-2C was identified in all the treated samples (albeit at different levels) in this study (Table 1), and previous studies have suggested that glutathionylation acts as a reversible protection mechanism for

preventing further irreversible oxidation formation on cysteines [78]. Based on the kinase activities and cysteine modifications detected in this study, it is possible that the inhibitory effect of GSSG and GSNO on BnSnRK2.6-2C may be caused by changes in the redox microenvironment around/in the protein. Such a possibility may deserve further investigation.

### Multiple cysteine modifications occurred in the redox-treated BnSnRK2.6-2C

ROS or NO is known to induce redox PTMs in plant proteins [79]. It is also well known that many thiol modifications are unstable and can be dynamically changed to other modifications. Protein thiols can be easily oxidized to sulfenic acids (RSOH), which serve as intermediates to other types of oxidations such as disulfides, sulfinic acids ($RSO_2H$), and sulfonic acids ($RSO_3H$) [80–82]. Protein RSOH has also been demonstrated to be a substrate for S-glutathionylation formation induced by GSSG and GSH [83–85]. GSNO used in this study is usually considered to be a NO donor for S-nitrosylation [14]. Here we found that GSNO caused S-glutathionylation of BnSnRK2.6-2C, and such PTM was previously found in other proteins [79,85,86], but it is the first time in a SnRK2 kinase.

Given the dynamic and complicated interconversions among different cysteine modifications, we designed a multiple-step workflow. It allowed not only to detect the final mBBr labeling, but also to monitor the changes induced by the redox treatments (Fig. 4, Fig. S4). For example, reversible cysteine oxidations of BnSnRK2.6-2C were found in both the control and oxidant-treated groups, suggesting that BnSnRK2.6-2C was originally partially oxidized. In addition, the presence of mBBr in the GSH control and the absence of S-glutathionylation in the DTT control (Table 1) indicate that the original reversible oxidation might be attributed to intra-protein disulfide bond [86]. After oxidant treatments of BnSnRK2.6-2C, our MS-based method also identified an increase in $RSO_3H$, an important irreversible modification that was hard to detect and largely neglected in previous studies [87–89]. Moreover, the identification of S-glutathionylation with a large number of peptide spectrum matches (PSMs) in all the treatment groups and the GSH control (Fig. 4D, Fig. S4, Table 1) confirmed the contributions of GSSG, GSH, and GSNO to S-glutathionylation formation and provided further evidence that S-glutathionylation may not be fully reducible by Grx.

Our data confirm that the configuration of cysteine residues affects the accessibility and thus reactivity
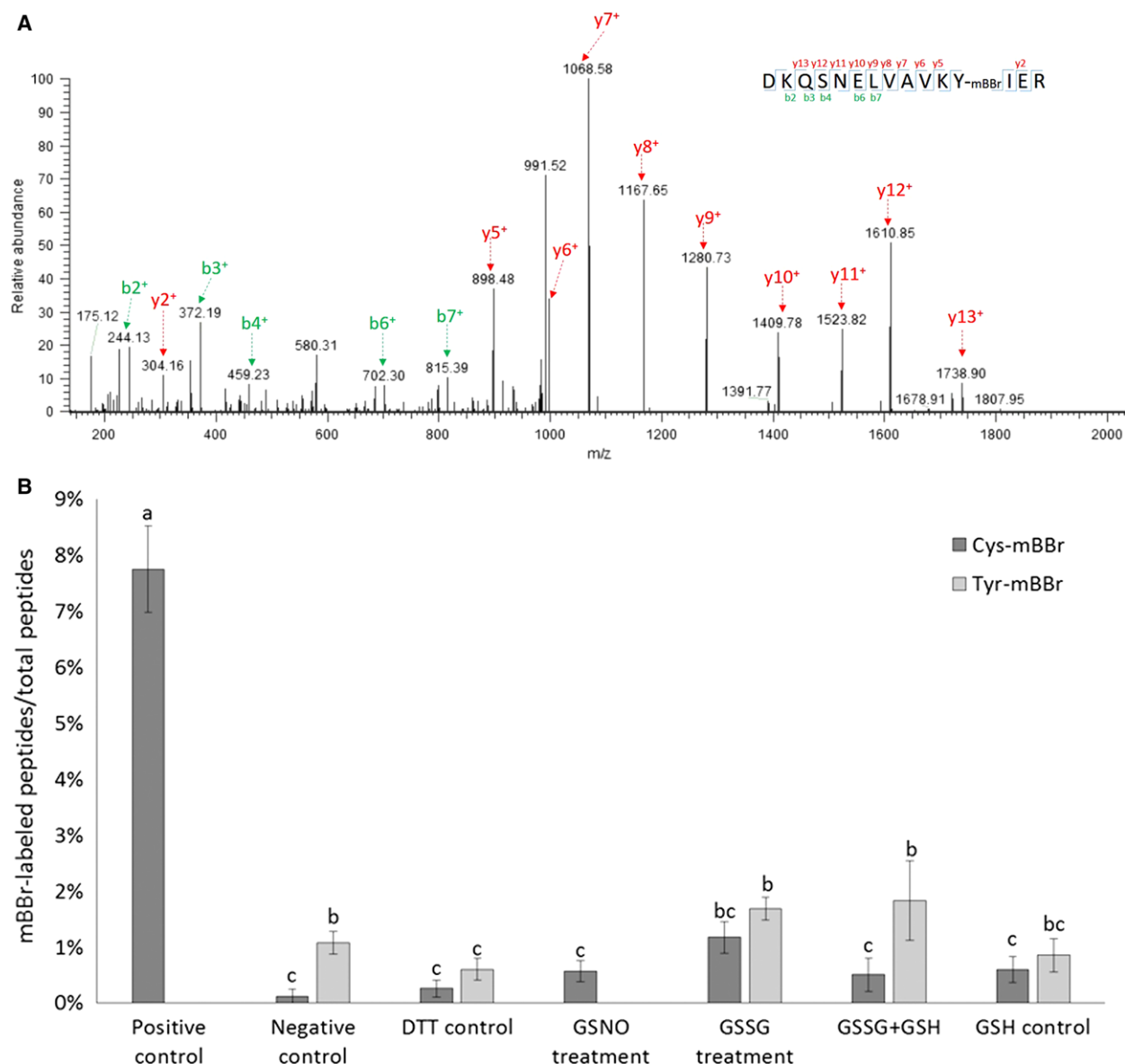
**Fig. 5.** Detection of peptides containing mBBr-labeled tyrosine residues by LC-MS/MS. (A) MS/MS spectrum of a peptide-containing mBBr-labeled Y51 of BnSnRK2.6-2C. MS/MS ions used for peptides identification were labeled. (B) Proportion of peptides with mBBr-labeled tyrosine and cysteine residues to total peptides detected in different redox treatments. Four replicates were used for statistical analysis, Duncan method was used in one-way ANOVA analysis, $P < 0.05$, and standard errors were indicated by error bars.

with redox reagents. For example, C159-containing peptides were detected with abundant PSMs and diverse PTMs compared to other cysteine-containing peptides. Interestingly, C159 is the only cysteine residue located in the flexible activation loop (Fig. 1) [60], and its location adjacent to the catalytic DFG sequence suggests this cysteine may play an important role in modulating kinase activity under different redox status. The second cysteine-containing peptide that we observed contains C107, which resides at the

outer surface. A previous study indicated that C137 in AtOST1 is modified with S-nitrosylation [14], but it was not detected in the BnSnRK2.6-2C (Table 1).

MS-based proteomics approaches have been used to identify redox-regulated thiol modifications with different cysteine-tagging techniques such as isotope-coded affinity tagging (ICAT) [22,89], cysteine reactive tandem mass tagging (cysTMT) [90,91], and iodoacetyl tandem mass tagging (iodoTMT) [92,93]. In spite of the rapid progress in discovering proteins with specific redox

PTMs in response to biotic or abiotic stresses [21,94–97], only limited studies have characterized the biological functions of the redox PTMs [14,15,78]. Different cysteine residues within a protein may occupy distinct redox microenvironment and thus be modified differently [86]. It is not clear how multiple redox PTMs (e.g., those identified in this work) coordinate to bring about functional changes. Future studies on redox PTM motifs, PTM cross talk, interaction of BnSnRK2.6-2C with redox proteins (e.g., thioredoxin and glutaredoxin), and fate of irreversibly oxidized BnSnRK2.6-2C will help unravel the complex mechanisms of the redox regulation and its functional significance.

### mBBr is MS/MS-compatible for redox modifications of cysteine and tyrosine residues

In this study, mBBr was chosen for indicating cysteine modification status, as well as identifying reversible thiol modifications (Figs 3 and 4, Figs S3 and S4) based on its use to specifically label cysteine thiols [98–100]. It was shown that inverse relationship between mBBr fluorescence and the concentration of GSNO used in the treatment of BnSnRK2.6-2C indicated corresponding cysteine modification levels (Fig. 3B,D). In addition, reversible thiol oxidations were detected using mBBr labeling in the MS analysis (Fig. 4A, Fig. S4). However, when using mBBr for detecting cysteine modification in GSSG-treated BnSnRK2.6-2C, the fluorescence showed little difference between controls and GSSG-treated samples (Fig. 3C,E), despite cysteine modifications being identified by MS/MS in those samples (Fig. 4, Fig. S4, Table 1). Here we detected mBBr labeling of tyrosine residues, which may explain the above observation. mBBr was shown to have lower affinity to tyrosine residues than cysteine residues, and Tyr-mBBr yields less fluorescence than Cys-mBBr [65]. Because of weaker fluorescence and reverse labeling methods, the influence of Tyr-mBBr may not be strong on the 2D gels used in previous proteomics work [98–100]. There are 11 tyrosine residues and six cysteine residues in the purified BnSnRK2.6-2C, fluorescence of Tyr-mBBr may influence the results of GSSG treatments (Figs 3C,E and 5B). Our detection of peptides with mBBr-labeled tyrosine residues by MS/MS (Fig. 5A, Fig. S5) suggests that the utility of mBBr as a tyrosine label may be considered in the future.

### Summary

In this study, recombinant BnSnRK2.6-2C displayed redox-regulated autophosphorylation activity. Oxidants GSSG and GSNO inhibited the activity of BnSnRK2.6-2C in a dose-dependent manner, and the inhibition was reversible. The forward labeling coupled with mBBr and reverse labeling coupled with MS analysis showed that multiple cysteine modifications including sulfonic acids and glutathionylation were formed under GSNO and GSSG treatments, and that C159 in the activation loop showed sensitivity to various modifications. mBBr can be used as a stable thiol label for evaluating cysteine redox status using LC-MS/MS. However, our MS data also revealed that mBBr-labeled tyrosine residues, and thus, caution is needed when interpreting the mBBr fluorescence data. Since the BnSnRK2.6-2C shares similar amino acid sequence with AtOST1 and both can be induced by similar stimuli such as ABA or drought [48], it is highly likely that redox regulation of BnSnRK2.6-2C may affect the guard cell processes known to be regulated by AtOST1, including cytosolic $Ca^{2+}$ concentration changes [9–12], ROS production [76], anion and potassium efflux [26,36–41], leading to stomatal closure (Fig. 6). This report of the different thiol modifications detected in the BnSnRK2.6-2C will facilitate future studies of the biological implications of the redox PTMs and their cross talk with kinase phosphorylation sites and activities.

## Materials and methods

### Sequence alignment and protein structure prediction

The sequence of *OST1* from Arabidopsis (*AtOST1*) was obtained from the Arabidopsis Information Resource (TAIR, http://www.arabidopsis.org/), the cDNA of *B. napus SnRK2.6-2A* and *SnRK2.6-2C* were identified in our previous work [48], and OST1 sequences of other species were retrieved according to previous studies [42–45,53]. Sequences were aligned by ClustalW [101], and the conserved domains were identified as previously described [59]. Sequence identity was calculated using the LALIGN program (http://www.ch.embnet.org/software/LALIGN_form.html). Protein tertiary structure was predicted using the RaptorX structure prediction server (http://raptorx.uchicago.edu/) [102], and the template for modeling was downloaded from the Protein Data Bank [103]. The Swiss PDB Viewer (http://spdbv.vital-it.ch) was used for analyzing the predicted protein structure.

### RNA extraction, cDNA synthesis, and gene cloning

Guard cell protoplasts (GCPs) were isolated as previously described [104]. Total RNA of *B. napus* GCPs was
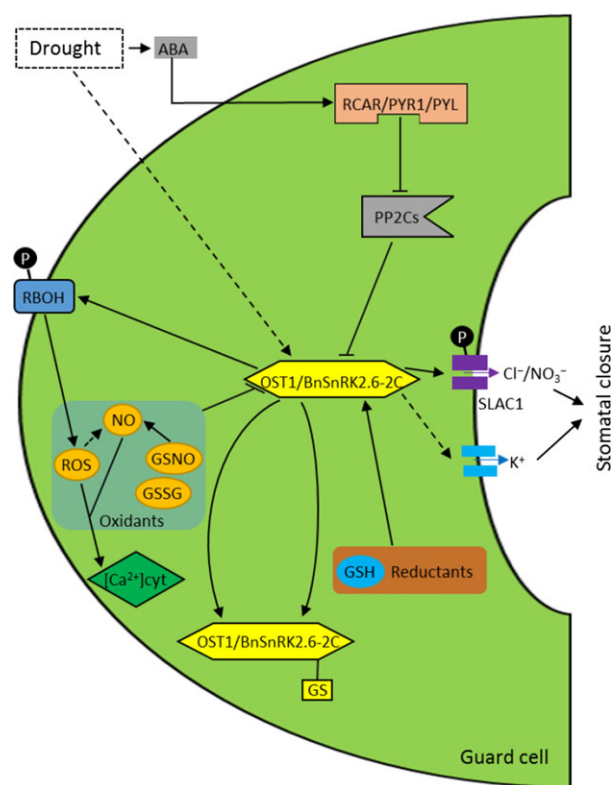
**Fig. 6.** Simplified diagram depicting how redox regulation of BnSnRK2.6-2C may affect guard cell processes leading to stomatal closure. Direct and indirect processes are indicated by solid and dashed lines, respectively.

extracted with a RNeasy® plant mini kit (Qiagen, USA) according to the manufacturer's protocol. A NanoDrop® 1000 spectrometer (Thermo Fisher Scientific Inc., USA) was used for checking RNA quality and quantity. The GoScript™ reverse transcription system (Promega, USA) was used for cDNA synthesis in a 20 μL reaction mixture using 1 μg of total RNA with random primers following the manufacturer's protocol. PCR amplification was carried out with the following primers: BnOST1.12F, 5′-CGC*GGATCC*GCGATG GATCGACCAGCAGTG-3′ with *Bam*H I site (italicized and underscored) and BnOST1.12R-X, 5′-CCG*CTCGAG*CGG CATTGCGTACACGATCTCTC-3′ with *Xho* I site. Q5® Hot Start High-Fidelity DNA Polymerase (New England Biolabs, USA) was used for PCR product following the manufacturer's protocol. PCR products were cloned using the StrataClone Blunt PCR Cloning Kit (Stratagene, USA), and their sequences were confirmed through sequencing.

## Recombinant BnSnRK2.6-2C expression and purification

The cloned *BnSnRK2.6-2C* described above and the pET28a expression vector (Novagen, USA) were double-

digested with *Bam*H I-HF and *Xho* I (New England Biolabs, USA), and the resulting gene fragment and linearized vector were ligated by T$_4$ DNA Ligase (New England Biolabs, USA). The constructs were transformed into *Escherichia coli* strain BL21 (DE3) for protein expression. Positive colonies were first growing in LB medium (0.5% w/v yeast extract, 1% w/v NaCl, 1% w/v tryptone) supplemented with 50 μg·mL$^{-1}$ kanamycin at 37 °C to OD$_{600}$ of 0.6, and then, the expression of recombinant BnSnRK2.6-C was induced with 1 mM isopropyl-beta-D-thiogalactopyranoside (IPTG) at 37 °C for 4 h. Recombinant his-tagged protein was purified using a Midi PrepEase® kit (Affymetrix/USB, USA) following the manufacturer's protocol. For kinase assays and mBBr labeling experiments, the recombinant BnSnRK2.6-2C was dialyzed at 4 °C overnight in 25 mM Tris/HCl pH 7.5 containing 0.5 mM DTT and 100 μM phenylmethanesulfonyl fluoride, and then washed with a 3 kD cutoff ultra-filtration unit (Millipore, USA). Bradford protein assay (Bio-Rad Laboratories Inc., USA) was used for determining protein concentration with bovine serum albumin as a standard [77].

## Redox treatment and in-solution kinase assay

The purified BnSnRK2.6-2C protein was aliquoted into ~ 1.5 μg for each treatment. Protein aliquots were treated with 0.3, 1, and 3 mM oxidant (GSNO or GSSG) in a volume of 40 μL for 15 min, and then incubated with either 10 mM DTT or GSH and/or 1 unit of Grx (Sigma-Aldrich Co., USA) for an additional 20 min. The amount of GSH in the treatments depended on the protein quantity, and a ratio of 1 mM GSH to 1 μg protein was used. All the treatments were performed at room temperature. Kinase activity assays were conducted as previously described [77]. Briefly, 20 μL of sample was incubated with an equal volume of kinase reaction buffer (50 mM Tris/HCl, pH 7.5, 10 mM MnCl$_2$, 2 μM ATP and 2 μCi [γ-$^{32}$P] ATP (PerkinElmer, USA)) at 30 °C for 30 min. The reaction was stopped by adding SDS/PAGE sample loading buffer, and the mixtures were incubated at 100 °C for 5 min. Samples were separated on SDS/PAGE, and the bands of interest were visualized by Coomassie Brilliant Blue R-250 (CBB) staining as described previously [77]. The activity of BnSnRK2.6-2C in the gels was determined by autoradiography. Four independent replicates of kinase assay were used for confirming the effects caused by GSNO or GSSG.

## Cysteine modification analysis using mBBr labeling

Aliquots of 3 μg recombinant BnSnRK2.6-2C were treated with 1 mM or 3 mM GSNO or 3 mM GSSG and reductants as described above. Redox-treated proteins were labeled with 0.2 mg of mBBr (Thermo Fisher Scientific Inc., USA)

dissolved in acetonitrile in the dark at room temperature for 1 h. Excess mBBr was removed by dichloromethane extraction. After addition of 200 μL dichloromethane, each sample was vortexed and centrifuged at 11 956 *g* for 2 min, and the dichloromethane in the lower phase was removed. This was repeated three times. IAM at a final concentration of 100 mM was used for blocking the remaining free thiol groups at 37 °C for 1 h in the dark. Proteins were separated on 12% SDS/PAGEs, and the gels were first washed with trichloroacetic acid for 1 h, and then washed with 10% acetic acid (v/v) and 40% methanol (v/v) overnight [105]. The labeling of mBBr was determined by imaging the gel under UV light [106], and the gels were then stained with CBB to estimate the protein amount. ImageJ (https://imagej.nih.gov/ij/index.html) was used for image analysis, and the relative fluorescence signals from mBBr labeling were normalized to the protein amount indicated by CBB staining. Three independent replicates were used for statistical analysis, and the Duncan method was used for one-way ANOVA analysis, with $P < 0.05$ as a significance cutoff.

## LC-MS/MS identification of cysteine modifications

A reverse labeling strategy for BnSnRK2.6-2C cysteine modification analysis is detailed in Fig. S3. Aliquots of BnSnRK2.6-2C (~ 3 μg) were incubated with 3 mM GSSG or GSNO for 30 min to react with responsive free thiol groups, and the remaining free thiols were subsequently alkylated with 100 mM IAM. Next, the samples were treated for 30 min with DTT (GSNO- and GSSG-treated samples) or GSH together with Grx (GSSG-treated samples), followed by labeling with mBBr as described above. To test the validity of the labeling workflow, the protein aliquots were initially fully reduced with DTT and were then labeled with mBBr directly as a positive control. For the negative control, blocking of the DTT-reduced free thiols with IAM was performed before the mBBr labeling. Another two controls consisted of an IAM blocking step, a reducing step with either DTT or GSH and Grx, and an mBBr labeling step, for testing effects of reductants only. Excessive mBBr was removed by the dichloromethane extraction described above, and the samples were digested with a modified trypsin (1 : 1 w/w) (Promega, USA) at 37 °C for 12 h. The digestion was terminated by adding 0.1% formic acid, and the tryptic peptides were then lyophilized [93]. The resulting samples were cleaned up by solid-phase extraction with ZipTip (Millipore, USA) according to the manufacturer's instructions.

The peptides were dissolved in 0.1% formic acid and then subjected to LC-MS/MS analysis. The scan range of the precursor ions on the Q Exactive Plus (Thermo Fisher Scientific Inc., USA) was set as 400–2000 m/z, and a top 20 data-dependent acquisition method was used for MS/MS [93]. The acquired MS/MS spectra were searched against a *B. napus* database (http://www.genoscope.cns.fr/brassicanapus/data/) with an additional sequence of the recombinant BnSnRK2.6-2C using Mascot (v2.4, Matrix Science, UK). The following dynamic modifications on the indicated amino acid residues were added: phosphorylation (STY), mBBr (CY), carbamidomethyl (C), nitrosylation (C), glutathionylation (C), oxidation (M, C), and formation of sulfinic acid and sulfonic acid (C). Other parameters were set as previously described [107]. To quantify the abundance of peptides with various modifications, the number of PSMs for identifying the modified peptides was calculated. These numbers were divided by the total PSMs for all the peptides of BnSnRK2.6-2C to normalize the relative abundance across different samples.

## Acknowledgements

## Author contributions

SC, MJY, and TZ planned the experiments; TM, MJY, LL, and WYS performed the experiments; TM, ACH, JK, and WS analyzed data; all the authors contributed to the writing of the manuscript, and ACH and SC finalized the manuscript.

## References

1 Casson SA and Hetherington AM (2010) Environmental regulation of stomatal development. *Curr Opin Plant Biol* **13**, 90–95.

2 Fujita M, Fujita Y, Noutoshi Y, Takahashi F, Narusaka Y, Yamaguchi-Shinozaki K and Shinozaki K (2006) Crosstalk between abiotic and biotic stress responses: a current view from the points of convergence in the stress signaling networks. *Curr Opin Plant Biol* **9**, 436–442.

3 Assmann SM (1993) Signal transduction in guard cells. *Annu Rev Cell Biol* **9**, 345–375.

4 Fedoroff NV (2002) Cross-talk in abscisic acid signaling. *Sci STKE* **2002**, re10.

5 Guzel Deger A, Scherzer S, Nuhkat M, Kedzierska J, Kollist H, Brosche M, Unyayar S, Boudsocq M, Hedrich R and Roelfsema MR (2015) Guard cell SLAC1-type anion channels mediate flagellin-induced stomatal closure. *New Phytol* **208**, 162–173.

6 Li S, Assmann SM and Albert R (2006) Predicting essential components of signal transduction networks: a dynamic model of guard cell abscisic acid signaling. *PLoS Biol* **4**, e312.

7 Schroeder JI, Kwak JM and Allen GJ (2001) Guard cell abscisic acid signalling and engineering drought hardiness in plants. *Nature* **410**, 327–330.

8 Munemasa S, Oda K, Watanabe-Sugimoto M, Nakamura Y, Shimoishi Y and Murata Y (2007) The coronatine-insensitive 1 mutation reveals the hormonal signaling interaction between abscisic acid and methyl jasmonate in Arabidopsis guard cells, Specific impairment of ion channel activation and second messenger production. *Plant Physiol* **143**, 1398–1407.

9 Zhu M, Dai S and Chen S (2012) The stomata frontline of plant interaction with the environment-perspectives from hormone regulation. *Front Biol* **7**, 96–112.

10 Neill SJ, Desikan R, Clarke A and Hancock JT (2002) Nitric oxide is a novel component of abscisic acid signaling in stomatal guard cells. *Plant Physiol* **128**, 13–16.

11 Pei ZM, Murata Y, Benning G, Thomine S, Klusener B, Allen GJ, Grill E and Schroeder JI (2000) Calcium channels activated by hydrogen peroxide mediate abscisic acid signalling in guard cells. *Nature* **406**, 731–734.

12 Saito N, Nakamura Y, Mori IC and Murata Y (2009) Nitric oxide functions in both methyl jasmonate signaling and abscisic acid signaling in Arabidopsis guard cells. *Plant Signal Behav* **4**, 119–120.

13 Konopka-Postupolska D, Clark G, Goch G, Debski J, Floras K, Cantero A, Fijolek B, Roux S and Hennig J (2009) The role of annexin 1 in drought stress in Arabidopsis. *Plant Physiol* **150**, 1394–1410.

14 Wang P, Du Y, Hou YJ, Zhao Y, Hsu CC, Yuan F, Zhu X, Tao WA, Song CP and Zhu JK (2015) Nitric oxide negatively regulates abscisic acid signaling in guard cells by S-nitrosylation of OST1. *Proc Natl Acad Sci USA* **112**, 613–618.

15 Mohapatra S and Mittra B (2016) Protein glutathionylation protects wheat (*Triticum aestivum* Var. Sonalika) against *Fusarium* induced oxidative stress. *Plant Physiol Biochem* **109**, 319–325.

16 Di Simplicio P, Franconi F, Frosali S and Di Giuseppe D (2003) Thiolation and nitrosation of cysteines in biological fluids and cells. *Amino Acids* **25**, 323–339.

17 Finkel T (2003) Oxidant signals and oxidative stress. *Curr Opin Cell Biol* **15**, 247–254.

18 Tonks NK (2005) Redox redux: revisiting PTPs and the control of cell signaling. *Cell* **121**, 667–670.

19 Lang Z and Zuo J (2015) Say "NO" to ABA signaling in guard cells by S-nitrosylation of OST1. *Sci China Life Sci* **58**, 313.

20 Gould KS, Lamotte O, Klinguer A, Pugin A and Wendehenne D (2003) Nitric oxide production in tobacco leaf cells: a generalized stress response? *Plant, Cell Environ* **26**, 1851–1862.

21 Dixon DP, Skipsey M, Grundy NM and Edwards R (2005) Stress-induced protein S-glutathionylation in Arabidopsis. *Plant Physiol* **138**, 2233–2244.

22 Zhu M, Zhu N, Song WY, Harmon AC, Assmann SM and Chen S (2014) Thiol-based redox proteins in abscisic acid and methyl jasmonate signaling in *Brassica napus* guard cells. *Plant J* **78**, 491–515.

23 Jin X, Wang RS, Zhu M, Jeon BW, Albert R, Chen S and Assmann SM (2013) Abscisic acid-responsive guard cell metabolomes of Arabidopsis wild-type and gpa1 G-protein mutants. *Plant Cell* **25**, 4789–4811.

24 Wang P and Song CP (2008) Guard-cell signalling for hydrogen peroxide and abscisic acid. *New Phytol* **178**, 703–718.

25 Cutler SR, Rodriguez PL, Finkelstein RR and Abrams SR (2010) Abscisic acid: emergence of a core signaling network. *Annu Rev Plant Biol* **61**, 651–679.

26 Geiger D, Scherzer S, Mumm P, Stange A, Marten I, Bauer H, Ache P, Matschi S, Liese A, Al-Rasheid KA *et al.* (2009) Activity of guard cell anion channel SLAC1 is controlled by drought-stress signaling kinase-phosphatase pair. *Proc Natl Acad Sci USA* **106**, 21425–21430.

27 Gonzalez-Guzman M, Pizzio GA, Antoni R, Vera-Sirera F, Merilo E, Bassel GW, Fernandez MA, Holdsworth MJ, Perez-Amador MA, Kollist H *et al.* (2012) Arabidopsis PYR/PYL/RCAR receptors play a major role in quantitative regulation of stomatal aperture and transcriptional response to abscisic acid. *Plant Cell* **24**, 2483–2496.

28 Sato A, Sato Y, Fukao Y, Fujiwara M, Umezawa T, Shinozaki K, Hibi T, Taniguchi M, Miyake H, Goto DB *et al.* (2009) Threonine at position 306 of the KAT1 potassium channel is essential for channel activity and is a target site for ABA-activated SnRK2/OST1/SnRK2.6 protein kinase. *Biochem J* **424**, 439–448.

29 Fujii H, Chinnusamy V, Rodrigues A, Rubio S, Antoni R, Park SY, Cutler SR, Sheen J, Rodriguez PL and Zhu JK (2009) *In vitro* reconstitution of an abscisic acid signalling pathway. *Nature* **462**, 660–664.

30 Fujii H, Verslues PE and Zhu JK (2007) Identification of two protein kinases required for abscisic acid regulation of seed germination, root growth, and gene expression in *Arabidopsis*. *Plant Cell* **19**, 485–494.

31 Kobayashi Y, Yamamoto S, Minami H, Kagaya Y and Hattori T (2004) Differential activation of the rice sucrose nonfermenting1-related protein kinase2 family by hyperosmotic stress and abscisic acid. *Plant Cell* **16**, 1163–1177.

32 Ma Y, Szostkiewicz I, Korte A, Moes D, Yang Y, Christmann A and Grill E (2009) Regulators of PP2C phosphatase activity function as abscisic acid sensors. *Science* **324**, 1064–1068.

33 Park SY, Fung P, Nishimura N, Jensen DR, Fujii H, Zhao Y, Lumba S, Santiago J, Rodrigues A, Chow TF *et al.* (2009) Abscisic acid inhibits type 2C protein phosphatases via the PYR/PYL family of START proteins. *Science* **324**, 1068–1071.

34 Furihata T, Maruyama K, Fujita Y, Umezawa T, Yoshida R, Shinozaki K and Yamaguchi-Shinozaki K (2006) Abscisic acid-dependent multisite phosphorylation regulates the activity of a transcription activator AREB1. *Proc Natl Acad Sci USA* **103**, 1988–1993.

35 Sirichandra C, Davanture M, Turk BE, Zivy M, Valot B, Leung J and Merlot S (2010) The Arabidopsis ABA-activated kinase OST1 phosphorylates the bZIP transcription factor ABF3 and creates a 14-3-3 binding site involved in its turnover. *PLoS ONE* **5**, e13935.

36 Brandt B, Brodsky DE, Xue S, Negi J, Iba K, Kangasjarvi J, Ghassemian M, Stephan AB, Hu H and Schroeder JI (2012) Reconstitution of abscisic acid activation of SLAC1 anion channel by CPK6 and OST1 kinases and branched ABI1 PP2C phosphatase action. *Proc Natl Acad Sci USA* **109**, 10593–10598.

37 Hayashi M, Inoue S, Takahashi K and Kinoshita T (2011) Immunohistochemical detection of blue light-induced phosphorylation of the plasma membrane H$^+$-ATPase in stomatal guard cells. *Plant Cell Physiol* **52**, 1238–1248.

38 Lee SC, Lan W, Buchanan BB and Luan S (2009) A protein kinase-phosphatase pair interacts with an ion channel to regulate ABA signaling in plant guard cells. *Proc Natl Acad Sci USA* **106**, 21419–21424.

39 Negi J, Matsuda O, Nagasawa T, Oba Y, Takahashi H, Kawai-Yamada M, Uchimiya H, Hashimoto M and Iba K (2008) CO$_2$ regulator SLAC1 and its homologues are essential for anion homeostasis in plant cells. *Nature* **452**, 483–486.

40 Vahisalu T, Kollist H, Wang YF, Nishimura N, Chan WY, Valerio G, Lamminmaki A, Brosche M, Moldau H, Desikan R *et al.* (2008) SLAC1 is required for plant guard cell S-type anion channel function in stomatal signalling. *Nature* **452**, 487–491.

41 Xue S, Hu H, Ries A, Merilo E, Kollist H and Schroeder JI (2011) Central functions of bicarbonate in S-type anion channel activation and OST1 protein kinase in CO$_2$ signal transduction in guard cell. *EMBO J* **30**, 1645–1658.

42 Vilela B, Morenocortés A, Rabissi A, Leung J, Pagès M and Lumbreras V (2013) The maize OST1 kinase homolog phosphorylates and regulates the maize SNAC1-type transcription factor. *PLoS ONE* **8**, e58105.

43 Shi K, Li X, Zhang H, Zhang G, Liu Y, Zhou Y, Xia X, Chen Z and Yu J (2015) Guard cell hydrogen peroxide and nitric oxide mediate elevated CO$_2$-induced stomatal movement in tomato. *New Phytol* **208**, 342–353.

44 Song X, Ohtani M, Hori C, Takebayasi A, Hiroyama R, Rejab NA, Suzuki T, Demura T, Yin T and Yu X (2015) Physical interaction between SnRK2 and PP2C is conserved in *Populus trichocarpa*. *Plant Biotechnol* **15**, 359–364.

45 Wang M, Yuan F, Hao H, Zhang Y, Zhao H, Guo A, Hu J, Zhou X and Xie CG (2013) BolOST1, an ortholog of Open Stomata 1 with alternative splicing products in *Brassica oleracea*, positively modulates drought responses in plants. *Biochem Biophys Res Comm* **442**, 214–220.

46 Ye W, Adachi Y, Munemasa S, Nakamura Y, Mori IC and Murata Y (2015) Open Stomata 1 kinase is essential for yeast elicitor-induced stomatal closure in Arabidopsis. *Plant Cell Physiol* **56**, 1239.

47 Anastasia M, Hanumakumar B, Alfonso MP, Mimi HS, Koh I, Schroeder JI and Maria IN (2015) The HT1 protein kinase is essential for red light-induced stomatal opening and genetically interacts with OST1 in red light and CO2-induced stomatal movement responses. *New Phytol* **208**, 1126–1137.

48 Yoo MJ, Ma T, Zhu N, Liu L, Harmon AC, Wang Q and Chen S (2016) Genome-wide identification and homeolog-specific expression analysis of the SnRK2 genes in *Brassica napus* guard cells. *Plant Mol Biol* **91**, 211–227.

49 Wang X, Wu D, Yang Q, Zeng J, Jin G, Chen ZH, Zhang G and Dai F (2016) Identification of mild freezing shock response pathways in barley based on transcriptome profiling. *Front Plant Sci* **7**, 106.

50 Huang Z, Tang J, Duan W, Wang Z, Song X and Hou X (2015) Molecular evolution, characterization, and expression analysis of SnRK2 gene family in Pak-choi (*Brassica rapa* ssp. chinensis), *Frontiers. Plant Sci* **6**, 879.

51 Ding Y, Li H, Zhang X, Xie Q, Gong Z and Yang S (2015) OST1 kinase modulates freezing tolerance by enhancing ICE1 stability in Arabidopsis. *Dev Cell* **32**, 278.

52 Nakashima K, Fujita Y, Kanamori N, Katagiri T, Umezawa T, Kidokoro S, Maruyama K, Yoshida T, Ishiyama K and Kobayashi M (2009) Three Arabidopsis SnRK2 protein kinases, SRK2D/SnRK2.2, SRK2E/SnRK2.6/OST1 and SRK2I/SnRK2.3, involved in ABA signaling are essential for the control of seed development and dormancy. *Plant Cell Physiol* **50**, 1345–1363.

53 Han Y, Dang R, Li J, Jiang J, Zhang N, Jia M, Wei L, Li Z, Li B and Jia W (2015) FaSnRK2.6, an ortholog of OPEN STOMATA 1, is a Negative regulator of strawberry fruit development and ripening. *Plant Physiol* **167**, 915–930.

54 Balmant KM, Zhang T and Chen S (2016) Protein phosphorylation and redox modification in stomatal guard cells. *Front Physiol* **7**, 26.

55 Zhang T, Chen S and Harmon AC (2014) Protein phosphorylation in stomatal movement. *Plant Signal Behav* **9**, e972845.

56 Fujii H and Zhu JK (2012) Osmotic stress signaling via protein kinases. *Cell Mol Life Sci* **69**, 3165–3173.

57 Mustilli AC, Merlot S, Vavasseur A, Fenzi F and Giraudat J (2002) Arabidopsis OST1 protein kinase mediates the regulation of stomatal aperture by abscisic acid and acts upstream of reactive oxygen species production. *Plant Cell* **14**, 3089–3099.

58 Sirichandra C, Gu D, Hu HC, Davanture M, Lee S, Djaoui M, Valot B, Zivy M, Leung J and Merlot S (2009) Phosphorylation of the Arabidopsis AtrbohF NADPH oxidase by OST1 protein kinase. *FEBS Lett* **583**, 2982.

59 Kulik A, Wawer I, Krzywinska E, Bucholc M and Dobrowolska G (2011) SnRK2 protein kinases–key regulators of plant response to abiotic stresses. *OMICS* **15**, 859–872.

60 Ng LM, Soon FF, Zhou XE, West GM, Kovach A, Suino-Powell KM, Chalmers MJ, Li J, Yong EL, Zhu JK *et al.* (2011) Structural basis for basal activity and autoactivation of abscisic acid (ABA) signaling SnRK2 kinases. *Proc Natl Acad Sci USA* **108**, 21259–21264.

61 Soon F-F, Ng L-M, Zhou XE, West GM, Kovach A, Tan ME, Suino-Powell KM, He Y, Xu Y and Chalmers MJ (2012) Molecular mimicry regulates ABA signaling by SnRK2 kinases and PP2C phosphatases. *Science* **335**, 85–88.

62 Chou C-C, Chiang B-Y, Lin JC-Y, Pan K-T, Lin C-H and Khoo K-H (2015) Characteristic tandem mass spectral features under various collision chemistries for site-specific identification of protein S-glutathionylation. *J Am Soc Mass Spectrom* **26**, 120–132.

63 Giustarini D, Milzani A, Aldini G, Carini M, Rossi R and Dalle-Donne I (2005) S-nitrosation versus S-glutathionylation of protein sulfhydryl groups by S-nitrosoglutathione. *Antioxid Redox Signal* **7**, 930–939.

64 Harris TK and Turner GJ (2002) Structural basis of perturbed pKa values of catalytic groups in enzyme active sites. *IUBMB Life* **53**, 85–98.

65 Hu L and Colman RF (1995) Monobromobimane as an affinity label of the xenobiotic binding site of rat glutathione S-transferase 3-3. *J Biol Chem* **270**, 21875–21883.

66 Liu Y and He C (2017) A review of redox signaling and the control of MAP kinase pathway in plants. *Redox Biol* **11**, 192–204.

67 Ortiz-Masia D, Perez-Amador MA, Carbonell J and Marcote MJ (2007) Diverse stress signals activate the C1 subgroup MAP kinases of Arabidopsis. *FEBS Lett* **581**, 1834–1840.

68 Chang R, Jang CJ, Branco-Price C, Nghiem P and Bailey-Serres J (2012) Transient MPK6 activation in response to oxygen deprivation and reoxygenation is mediated by mitochondria and aids seedling survival in Arabidopsis. *Plant Mol Biol* **78**, 109–122.

69 Gupta R and Luan S (2003) Redox control of protein tyrosine phosphatases and mitogen-activated protein kinases in plants. *Plant Physiol* **132**, 1149–1152.

70 Desikan R, Hancock JT, Ichimura K, Shinozaki K and Neill SJ (2001) Harpin induces activation of the Arabidopsis mitogen-activated protein kinases AtMPK4 and AtMPK6. *Plant Physiol* **126**, 1579–1587.

71 Jammes F, Song C, Shin D, Munemasa S, Takeda K, Gu D, Cho D, Lee S, Giordo R and Sritubtim S (2009) MAP kinases MPK9 and MPK12 are preferentially expressed in guard cells and positively regulate ROS-mediated ABA signaling. *Proc Natl Acad Sci* **106**, 20520–20525.

72 Shi B, Ni L, Liu Y, Zhang A, Tan M and Jiang M (2014) OsDMI3-mediated activation of OsMPK1 regulates the activities of antioxidant enzymes in abscisic acid signalling in rice. *Plant, Cell Environ* **37**, 341–352.

73 Xie G, Sasaki K, Imai R and Xie D (2014) A redox-sensitive cysteine residue regulates the kinase activities of OsMPK3 and OsMPK6 *in vitro*. *Plant Sci* **227**, 69–75.

74 Wang J, Ding H, Zhang A, Ma F, Cao J and Jiang M (2010) A novel mitogen-activated protein kinase gene in maize (Zea mays), ZmMPK3, is involved in response to diverse environmental cues. *J Integr Plant Biol* **52**, 442–452.

75 Lin F, Ding H, Wang J, Zhang H, Zhang A, Zhang Y, Tan M, Dong W and Jiang M (2009) Positive feedback regulation of maize NADPH oxidase by mitogen-activated protein kinase cascade in abscisic acid signalling. *J Exp Bot* **60**, 3221–3238.

76 Nie WF, Wang MM, Xia XJ, Zhou YH, Shi K, Chen Z and Yu JQ (2013) Silencing of tomato RBOH1 and MPK2 abolishes brassinosteroid-induced $H_2O_2$ generation and stress tolerance. *Plant, Cell Environ* **36**, 789–803.

77 Zhang T, Zhu M, Song W-Y, Harmon AC and Chen S (2015) Oxidation and phosphorylation of MAP kinase 4 cause protein aggregation. *Biochimi Biophys Acta* **1854**, 156–165.

78 Barrett WC, DeGnore JP, König S, Fales HM, Keng Y-F, Zhang Z-Y, Yim MB and Chock PB (1999) Regulation of PTP1B via glutathionylation of the active site cysteine 215. *Biochemistry* **38**, 6699–6705.

79 Navrot N, Finnie C, Svensson B and Hägglund P (2011) Plant redox proteomics. *J Proteomics* **74**, 1450–1462.

80 Nagy P and Ashby MT (2007) Reactive sulfur species: kinetics and mechanisms of the oxidation of cysteine by hypohalous acid to give cysteine sulfenic acid. *J Am Chem Soc* **129**, 14082–14091.

81 Cremlyn RJW (1996) *An Introduction to Organosulfur Chemistry*. Wiley, Chichester, New York.

82 Hamann M, Zhang T, Hendrich S and Thomas JA (2002) Quantitation of protein sulfinic and sulfonic acid, irreversibly oxidized protein cysteine sites in cellular proteins. *Methods Enzymol* **348**, 146–156.

83 Lind C, Gerdes R, Hamnell Y, Schuppe-Koistinen I, von Lowenhielm HB, Holmgren A and Cotgreave IA (2002) Identification of S-glutathionylated cellular proteins during oxidative stress and constitutive metabolism by affinity purification and proteomic analysis. *Arch Biochem Biophys* **406**, 229–240.

84 Johansson C, Lillig CH and Holmgren A (2004) Human mitochondrial glutaredoxin reduces S-glutathionylated proteins with high affinity accepting electrons from either glutathione or thioredoxin reductase. *J Biol Chem* **279**, 7537–7543.

85 Couturier J, Chibani K, Jacquot JP and Rouhier N (2013) Cysteine-based redox regulation and signaling in plants. *Front Plant Sci* **4**, 105.

86 Reddie KG and Carroll KS (2008) Expanding the functional diversity of proteins through cysteine oxidation. *Curr Opin Chem Biol* **12**, 746–754.

87 Sethuraman M, McComb ME, Huang H, Huang S, Heibeck T, Costello CE and Cohen RA (2004) Isotope-coded affinity tag (ICAT) approach to redox proteomics: identification and quantitation of oxidant-sensitive cysteine thiols in complex protein mixtures. *J Proteome Res* **3**, 1228–1233.

88 Hurd TR, Prime TA, Harbour ME, Lilley KS and Murphy MP (2007) Detection of reactive oxygen species-sensitive thiol proteins by redox difference gel electrophoresis: implications for mitochondrial redox signaling. *J Biol Chem* **282**, 22040–22051.

89 Fu C, Hu J, Liu T, Ago T, Sadoshima J and Li H (2008) Quantitative analysis of redox-sensitive proteome with DIGE and ICAT. *J Proteome Res* **7**, 3789–3802.

90 Parker J, Balmant K, Zhu F, Zhu N and Chen S (2015) cysTMTRAQ-An integrative method for unbiased thiol-based redox proteomics. *Mol Cell Proteomics* **14**, 237–242.

91 Zhang T, Zhu M, Zhu N, Strul JM, Dufresne CP, Schneider JD, Harmon AC and Chen S (2016) Identification of thioredoxin targets in guard cell enriched epidermal peels using cysTMT proteomics. *J Proteomics* **133**, 48–53.

92 Qu Z, Meng F, Bomgarden RD, Viner RI, Li J, Rogers JC, Cheng J, Greenlief CM, Cui J, Lubahn DB *et al*. (2014) Proteomic quantification and site-mapping of S-nitrosylated proteins using isobaric iodoTMT reagents. *J Proteome Res* **13**, 3200–3211.

93 Yin Z, Balmant K, Geng S, Zhu N, Zhang T, Dufresne C, Dai S and Chen S (2017) Bicarbonate induced redox proteome changes in Arabidopsis suspension cells. *Front Plant Sci* **8**, 58.

94 Fares A, Rossignol M and Peltier JB (2011) Proteomics investigation of endogenous S-nitrosylation in Arabidopsis. *Biochem Biophys Res Comm* **416**, 331–336.

95 Puyaubert J, Fares A, Reze N, Peltier JB and Baudouin E (2014) Identification of endogenously S-nitrosylated proteins in Arabidopsis plantlets: effect of cold stress on cysteine nitrosylation level. *Plant Sci* **215–216**, 150–156.

96 Hu J, Huang X, Chen L, Sun X, Lu C, Zhang L, Wang Y and Zuo J (2015) Site-specific nitrosoproteomic identification of endogenously S-nitrosylated proteins in Arabidopsis. *Plant Physiol* **167**, 1731–1746.

97 Camejo D, Romero-Puertas Mdel C, Rodriguez-Serrano M, Sandalio LM, Lazaro JJ, Jimenez A and Sevilla F (2013) Salinity-induced changes in S-nitrosylation of pea mitochondrial proteins. *J Proteomics* **79**, 87–99.

98 Wong JH, Balmer Y, Cai N, Tanaka CK, Vensel WH, Hurkman WJ and Buchanan BB (2003) Unraveling thioredoxin-linked metabolic processes of cereal starchy endosperm using proteomics. *FEBS Lett* **547**, 151–156.

99 Wong JH, Cai N, Balmer Y, Tanaka CK, Vensel WH, Hurkman WJ and Buchanan BB (2004) Thioredoxin targets of developing wheat seeds identified by complementary proteomic approaches. *Phytochemistry* **65**, 1629–1640.

100 Alvarez S, Zhu M and Chen S (2009) Proteomics of Arabidopsis redox proteins in response to methyl jasmonate. *J Proteomics* **73**, 30–40.

101 Thompson JD, Gibson TJ and Higgins DG (2002) *Multiple Sequence Alignment Using ClustalW and ClustalX*. John Wiley & Sons Inc, Hoboken, NJ.

102 Källberg M, Wang H, Wang S, Peng J, Wang Z, Lu H and Xu J (2012) Template-based protein structure modeling using the RaptorX web server. *Nat Protoc* **7**, 1511–1522.

103 Berman HM, Westbrook J, Feng Z, Gilliland G, Bhat TN, Weissig H, Shindyalov IN and Bourne PE (2000) The Protein Data Bank, 1999. *Int Tables Crystallogr* **67**, 675–684.

104 Zhu M, Dai S, McClung S, Yan X and Chen S (2009) Functional differentiation of *Brassica napus* guard cells and mesophyll cells revealed by comparative proteomics. *Mol Cell Proteomics* **8**, 752–766.

105 Cotgreave IA and Moldéus P (1986) Methodologies for the application of monobromobimane to the

simultaneous analysis of soluble and protein thiol components of biological systems. *J Biochem Biophys Methods* **13**, 231–249.

106 Alvarez S, Wilson GH and Chen S (2009) Determination of *in vivo* disulfide-bonded proteins in Arabidopsis. *J Chromatogr B* **877**, 101–104.

107 Yu B, Li J, Koh J, Dufresne C, Yang N, Qi S, Zhang Y, Ma C, Duong BV and Chen S (2016) Quantitative proteomics and phosphoproteomics of sugar beet monosomic addition line M14 in response to salt stress. *J Proteomics* **143**, 286–297.

## Supporting information

Additional Supporting Information may be found online in the supporting information tab for this article:

**Fig. S1.** Alignment of BnSnRK2.6-2C sequence with other OST1 homologs. (A) Sequence alignment of cDNA sequences of *BnSnRK2.6-2A*, *BnSnRK2.6-2C* and *AtOST1*. (B) Sequence alignment of amino acid sequences of functionally studied OST1s of different plant species. OST1 sequences of *Brassica oleracea* (BolOST1-1, GenBank ID: AHE78413.1), *Fragaria vesca* subsp. vesca (FaSnRK2.6, NCBI reference sequence: XP_004290308.1), *Solanum lycopersicum* (SolycOST1, NCBI reference sequence: XP_004230794.1), *Populus trichocarpa* (PtSnRK2.11, NCBI reference sequence: XP_002313835.1; PtSnRK2.12, NCBI reference sequence: XP_006384459.1) and *Zea mays* (ZmOST1, GenBank ID: ACG36261.1) were used for alignment together with AtOST1 and BnSnRK2.6-2C. The locations of cysteine residues are labeled with red boxes.

**Fig. S2.** Phosphorylation sites identification of BnSnRK2.6-2C by mass spectrometry. MS/MS spectra of peptides containing phosphorylated S29 (A), S43 (B), S71 (C), T146 (D), S164 (E), S166 (F), S167 and S171 (G), S175 (H,I), Y182 (I), S262 (J), and S267 (K) of BnSnRK2.6-2C detected by LC-MS/MS. MS/MS ions used for peptides identification were labeled.

**Fig. S3.** Diagram depicting monobromobimane (mBBr) labeling workflow to identify reversible oxidations of cysteine residues in BnSnRK2.6-2C and the positive and negative controls (Table 1 for results). Positive control: The protein was reduced with DTT, labeled with mBBr directly, and then treated with IAM. Negative control: DTT-reduced free thiols were blocked with IAM before the mBBr labeling. DTT control: The protein was blocked with IAM, then reduced with DTT and labeled with mBBr. GSH control: The protein was blocked with IAM, and then reduced with GSH and Grx, followed by mBBr labeling. GSNO, GSSG and GSSG + GSH treatments (reverse labeling): After the treatment, IAM was used to block the remaining free thiol groups. Reversibly oxidized cysteine residues were then reduced with DTT or GSH and Grx, followed by mBBr labeling.

**Fig. S4.** Identification of BnSnRK2.6-2C cysteine residue modifications in response to GSNO and GSSG treatments by mass spectrometry. MS/MS spectra of peptides containing C107 modified by IAM (A), mBBr (B), or glutathione group (C), C131 and C137 modified by IAM (D), C203 modified by IAM (E), C250 modified by IAM (F) or mBBr (G) in BnSnRK2.6-2C by LC-MS/MS. MS/MS ions used for peptides identification were labeled.

**Fig. S5.** Identification of peptides containing mBBr-labeled Y182 in BnSnRK2.6-2C. MS/MS ions used for peptides identification were labeled.